Epigenetic heterogeneity of the Notch signaling components in the human developing retina

Takahiro Nakayama[1], Masaharu Yoshihara[2], Satoru Takahashi[3,4]

[1] College of Medicine, School of Medicine and Health Sciences, University of Tsukuba
[2] Department of Primary Care and Medical Education, Institute of Medicine, University of Tsukuba
[3] Department of Anatomy and Embryology, Institute of Medicine, University of Tsukuba
[4] Transborder Medical Research Center, Institute of Medicine, University of Tsukuba

Article type
Article

Corresponding author
Masaharu Yoshihara, M.D. Ph.D.
Assistant Professor
Institute of Medicine, University of Tsukuba
(Postal code) 1-1-1 Tennodai, Tsukuba, Ibaraki, 305-8575, Japan
(Phone) 81-29-853-7516
(FAX) 81-29-853-6965
(E-mail) yoshihara.masahar.ly@alumni.tsukuba.ac.jp

E-mail addresses
Takahiro Nakayama: nakayama.takahiro.rp@alumni.tsukuba.ac.jp
Masaharu Yoshihara: yoshihara.masahar.ly@alumni.tsukuba.ac.jp
Satoru Takahashi: satoruta@md.tsukuba.ac.jp

ORCID IDs
Takahiro Nakayama: 0000-0002-4023-4560
Masaharu Yoshihara: 0000-0002-0212-0909
Satoru Takahashi: 0000-0002-8540-7760

Abstract
Notch signaling-mediated differentiation is dependent on the fine-tuned expression regulation. Especially, the diversification processes of the initially homogenous

undifferentiated cells were well-documented for this signaling pathway. Although this signaling pathway is involved in the development of mammalian retina, for example, it is unclear how the expression levels of the Notch signaling components were regulated. Here, we analyzed the publicly available datasets of single-cell RNA-seq and single-cell ATAC-seq from human fetus retina at days 53, 59 and 78 to examine the status of the mRNA expressions and chromatin accessibilities of the Notch signaling components. We found that Notch signaling components were expressed in the undifferentiated cells and that the chromatin accessibilities in those cells were different among themselves. This finding revealed the epigenetic heterogeneity among the differentiating cells during Notch signaling-driven cellular dynamics.

Introduction

Notch signaling pathway is essential for the development of nervous system including retina (1). Indeed, a transgenic mouse study revealed that most of the retinal cells were receiving Notch1 signaling (2). Along with inducing differentiation, this signaling pathway is known to generate the fine-grained cell arrangement of the differentiated cells from initial undifferentiated cells in *Drosophila* neurogenesis, for example (3). The lateral inhibition with feedback mechanism that is supported by low surface expression rate of the DSL ligands in the NOTCH signaling-receiving cells has been well-documented to generate this fine-grained pattern (4). Indeed, the oscillation of Dll1 (one of the mammalian DSL ligands) mRNA levels is critical in somitogenesis (5). Another computer simulation study suggested that the redundant expression of both DSL ligands and NOTCH receptors were essential for the generation of fine-grained pattern via ligand-receptor interaction (6). Importantly, initial homogeneity is assumed in the previous computer simulation studies (4) (6) (7).

Single-cell multi-omics has enabled genome-wide examination of mRNA expression (8) and chromatin accessibilities (9). Combining single-cell RNA-seq (scRNAseq) and single-cell ATAC-seq (scATACseq) reveals chromatin accessibilities of gene of interest in a specific cell population. For example, retina is composed of three layers (photoreceptor, bipolar cell, and retinal ganglion cell layers) intercalated with amacrine cells and horizontal cells. Since these differentiated cells arise from a single progenitor cell (multipotent progenitor cells, MPCs), it is important to distinguish the specific cell stages where Notch signaling is acting. Since the scRNAseq and scATACseq datasets from human fetus retinas (days 53, 59 and 78) were recently reported (10), in this study, the chromatin accessibilities in the differentiating cells were analyzed to examine the homogeneity in the Notch signaling components from an epigenetic perspective.

Results

scRNAseq and scATACseq analysis of day 53 fetus retina

We started with the dataset from the youngest fetus (day 53, d53). We carried out principal component analysis (PCA) followed by uniform manifold approximation and projection (UMAP) that generated seven clusters (Figure 1A). Unfortunately, two clusters were characterized with mitochondrial genes, suggesting that these cell populations represented dead cells (dead1 and dead2). The remaining cells were largely undifferentiated cells that were characterized with CCND1 (MPC marker) (11) or PLXNA2 (retinal progenitor cell marker, RPC) (12) (Figure 1B). One small cluster were characterized with POU4F2 (retinal ganglion cell marker, RGC) (11). In mammals, this signaling pathway is consisted of the five DSL ligands (JAG1, JAG2, DLL1, DLL3 and DLL4), the four NOTCH receptors (NOTCH 1-4) and several downstream target genes such as HES1, HES5, HEY1 and HEY2 (13). JAG1 and DLL1 were expressed in MPCs (Figure 1C) while NOTCH1, NOTCH2 and NOTCH3 were expressed in MPCs (Figure 1D). As expected, HES1 was expressed in MPCs (Figure 1E). Next, we analyzed scATACseq dataset from the same d53 fetus using ArchR package (21). We took an Iterative Latent Semantic Indexing (Iterative LSI)-based method for UMAP-based clustering that generated nine clusters. Since the scRNAseq analysis suggested NOTCH receptor expressions in the CCND1-expressing undifferentiated cells, we examined chromatin accessibilities near CCND1-coding site (100 kb on either side of the gene). The violin plot showed that the two clusters had high gene scores (C3 and C4; arrowheads) (Figure 1G). One of them (C3) also had a high gene score for JAG1 while the other (C4) had a low gene score owing to zero score in more than 25% of these cells (Figure 1H). Concerning the downstream target gene, HES1, both C3 and C4 clusters had high gene scores (Figure 1I). In summary, we observed heterogeneity in the chromatin accessibility near JAG1 among the undifferentiated cell populations (C3 and C4). The violin plots for the other Notch signaling components were available at Supplementary Fig. S1.

scRNAseq and scATACseq analysis of day 59 fetus retina

Then, we analyzed the dataset from the day 59 fetus (d59). PCA followed by UMAP clustering generated six clusters (Figure 2A). We used ELAVL4 (14), PLXNA2 (12). CPLX2 (15) and OTX2 (16) for the markers of RGCs, RPC, proliferating / amacrine cells (AMA) and the common progenitor cells for cone / rod (CON/ROD), respectively (Figure 2B). The AMA cluster co-expressed the DSL ligands (DLL 1-3), NOTCH1 and downstream target genes (HES5 and HEY1) (Figure 2C-2E). Iterative LSI-based method for UMAP-based clustering generated fifteen clusters. To our surprise, the cluster characteristics of the gene scores for CPLX2 and NOTCH1 differed because that for CPLX2 was high in the clusters 1-8 whereas

that for NOTCH1 was high in the clusters 10, 11, 13-15 (Figure 2G and 2H). The gene score for HES5 was heterogenous among the clusters 10, 11, 13-15 because the first quartile of the cluster 14 (arrowheads) was zero (Figure I). Therefore, the HES5 responsibleness for NOTCH1 signaling might be different among the clusters 10, 11, 13-15. The violin plots for the other Notch signaling components were available at Supplementary Fig. S2.

scRNAseq and scATACseq analysis of day 78 fetus retina

Finally, we analyzed the dataset from the day78 fetus (d78). PCA followed by UMAP clustering generated nine clusters (Figure 3A). We used MYBL1 (17) for the marker of RPC in addition to the other markers (CCND1, OTX2, ELAVL4 and PLXNA2) (Figure 3B). MPC1 were rich in the expression of NOTCH1, HES1 and HES5 whereas RPC3 were rich in the expression of DLL1, DLL4, NOTCH1 and HES5 (Figure 3C-3E). Iterative LSI-based method for UMAP-based clustering generated ten clusters where only cluster 6 (arrowheads) had high gene scores for CCND1, NOTCH1 and HES1, possibly because many cells had undergone differentiation at this developmental stage (Figure 3G-3I). Therefore, it was difficult to point out the heterogeneity in the Notch signaling components that was observed in d53 and d59. The violin plots for the other Notch signaling components were available at Supplementary Fig. S3.

Discussion

The patterning morphogenesis via Notch signaling pathway has been studied for decades and is thought to be mediated by fine-tuned regulation on the surface expression of Notch signaling components. The underlying molecular mechanism, however, is still unclear. For example, Mindbomb (MIB) affects the trafficking of DLS ligand proteins via ubiquitination (18). Only recently, an upstream epigenetic regulator, Stuxnet (stx), is reportedly promotes Notch receptor mRNA expression in *Drosophila* (19). It is, however, less-documented whether there is an epigenetic heterogeneity among the differentiating cells. In this study, we identified the heterogeneity of Notch signaling components among the undifferentiated cells at an epigenetic level that potentially impacts the transcriptional control of Notch signaling components. In addition, while the previous computer simulation studies assumed the initial homogeneity with fluctuation, this study questioned this assumption. Since our observation might focus on the middle of the retinal development, further examination is warranted using the samples at earlier developmental stages that are not currently available. In addition, the impact of this epigenetic heterogeneity on the patterning morphogenesis is a target of future studies.

There are several limitations in the present study. First, this study is an observational study

from the single sample at each developmental stage (d53, d59 and d78). Therefore, it is necessary to carry out additional sampling or interventional animal experiments to examine the validity of the information reported in this study. Second, the correlations between the mRNA expressions in scRNAseq and the gene scores in scATACseq were uncertain because we observed a situation where the gene score distributions were mismatched between CPLX2 (high in the clusters 1-8 and 11) and NOTCH1 (high in the clusters 11 and 13-15) in the d59 dataset. However, it is important to note that there the gene score levels for HES5 differed in the clusters where that for NOTCH1 was high (clusters 10, 11, 13-15), supporting the idea of heterogeneity. Third, without further examination, the idea of heterogeneity is not generalizable to other biological contexts where Notch signaling is in action.

Methods

The scRNAseq and scATACseq datasets for the human fetus retinas at days 53, 59 and 78 were downloaded from Gene Expression Omnibus (https://www.ncbi.nlm.nih.gov/geo/) (Accession Number GSE183684) (10). For the analysis of scRNA datasets, Seurat version 4.3.0.1 (20) was used in R version 4.3.1 (21) under macOS Ventura 13.4.1. Since the dataset d53 contained many dead cells with increased mitochondrial genes, the cells with less than three percent mitochondrial genes were selected for further analysis. After dimension reduction with PCA and clustering with UMAP, 2000 highly variable features across 2111 cells were finally used for the analysis. For the datasets d59 and d78, the threshold of percentage of mitochondrial genes were set to five. The numbers of the highly variable genes were set to 2000 and the final cell numbers analyzed were 5755 cells for the dataset d59 and 5997 cells for the dataset d78.

For the analysis of scATACseq dataset, ArchR (22) was used in R version 4.3.1 (21) under macOS Ventura 13.4.1. For the dataset d53, minimal TSS score was set to zero to collect enough number of the cells for the analysis. The other parameters were set to the default values. The numbers of cells analyzed were 9103, 7249 and 10399 for d53, d59 and d78, respectively. The numbers of median TSS were 9.499, 11.342 and 10.843 for d53, d59 and d78, respectively. The numbers of median Frags were 12522, 13996 and 10192 for d53, d59 and d78, respectively.

References

1. Chen, X. & Emerson, M. M. Notch signaling represses cone photoreceptor formation through the regulation of retinal progenitor cell states. *Sci. Rep.* **11**, 14525; 10.1038/s41598-021-93692-w (2021).
2. Yoshihara, M. *et al*. Generation of a Gal4-dependent gene recombination and

illuminating mouse. *Exp. Anim.* **71**, 385-390 (2022).

3. Heitzler, P. & Simpson, P. The choice of cell fate in the epidermis of Drosophila. *Cell.* **64**, 1083-1092 (1991).
4. Collier, J. R., Monk, N. A., Maini, P. K. & Lewis, J. H. Pattern formation by lateral inhibition with feedback: a mathematical model of delta-notch intercellular signalling. *J. Theor. Biol*. **183**, 429-446 (1996).
5. Shimojo, H. *et al*. Oscillatory control of Delta-like1 in cell interactions regulates dynamic gene expression and tissue morphogenesis. *Genes Dev*. **30**, 102-116 (2016)
6. Yoshihara, M. *et al*. Mathematical analysis of the effect of portal vein cells on biliary epithelial cell differentiation through the Delta-Notch signaling pathway. *BMC Res. Notes*. **14**, 243; 10.1186/s13104-021-05656-y (2021).
7. Sprinzak, D., Lakhanpal, A., LeBon, L., Garcia-Ojalvo, J. & Elowitz, M. B. Mutual inactivation of Notch receptors and ligands facilitates developmental patterning. *PLoS Comput. Biol*. **7**, e1002069; 10.1371/journal.pcbi.1002069 (2011).
8. Tang, F. *et al*. mRNA-Seq whole-transcriptome analysis of a single cell. *Nat. Methods*. **6**, 377-382 (2009).
9. Buenrostro, J. D. *et al*. Single-cell chromatin accessibility reveals principles of regulatory variation. *Nature*. **523**, 486-490 (2015).
10. Lyu, P. *et al*. Gene regulatory networks controlling temporal patterning, neurogenesis, and cell-fate specification in mammalian retina. *Cell Rep*. **37**, 109994; 10.1016/j.celrep.2021.109994 (2021).
11. Finkbeiner, C. *et al*. Single-cell ATAC-seq of fetal human retina and stem-cell-derived retinal organoids shows changing chromatin landscapes during cell fate acquisition. *Cell Rep*. **38**, 110294; 10.1016/j.celrep.2021.110294 (2022).
12. Emerson, S. E. *et al*. Identification of target genes downstream of semaphorin6A/PlexinA2 signaling in zebrafish. *Dev. Dyn*. **246**, 539-549 (2017).
13. Kopan, R. & Ilagan, M. X. The canonical Notch signaling pathway: unfolding the activation mechanism. *Cell*. **137**, 216-233 (2009).
14. Wu, F. *et al*. Single cell transcriptomics reveals lineage trajectory of retinal ganglion cells in wild-type and Atoh7-null retinas. *Nat. Commun*. **12**, 1465; 10.1038/s41467-021-21704-4 (2021).
15. Reim, K. *et al*. Aberrant function and structure of retinal ribbon synapses in the absence of complexin 3 and complexin 4. *J. Cell Sci*. **122**, 1352-1361 (2009).
16. Emerson, M. M., Surzenko, N., Goetz, J. J., Trimarchi, J. & Cepko, C. L. Otx2 and Onecut1 promote the fates of cone photoreceptors and horizontal cells and repress rod photoreceptors. *Dev. Cell*. **26**, 59-72 (2013).

17. Kaufman, M. L. *et al*. Transcriptional profiling of murine retinas undergoing semi-synchronous cone photoreceptor differentiation. *Dev. Biol*. **453**, 155-167 (2019).
18. Scavuzzo, M. A. *et al*. Pancreatic Cell Fate Determination Relies on Notch Ligand Trafficking by NFIA. *Cell Rep*. **25**, 3811-3827.e7; 10.1016/j.celrep.2018.11.078 (2018).
19. He, T. *et al*. Stuxnet fine-tunes Notch dose during development using a functional Polycomb response element. *Development*. **150**, dev201297; 10.1242/dev.201297 (2023).
20. Hao, Y. *et al*. Integrated analysis of multimodal single-cell data. *Cell*. **184**, 3573-3587 (2021).
21. R Core Team (2023). _R: A Language and Environment for Statistical Computing_. R Foundation for Statistical Computing, Vienna, Austria. <https://www.R-project.org/>.
22. Granja, J. M. *et al*. ArchR is a scalable software package for integrative single-cell chromatin accessibility analysis. *Nat. Genet*. **53**, 403-411 (2021).

Acknowledgements

This work was supported by JSPS KAKENHI (Grant Numbers JP23K14429 and JP22K20734 to MY) and YOKOYAMA Foundation for Clinical Pharmacology (Grant Number YRY-2207 to MY).

Author contributions

TN carried out analysis and wrote the manuscript. MY helped analysis and revised the manuscript. ST substantially revised the manuscript.

Competing Interests

The authors declare no competing interests.

Data availability

All the codes and results used or generated in the current study is available at our GitHub repository (https://github.com/nakayama-takahiro/i-atac).

Ethics declaration

This study did not generate any original data from animal experiments and human subjects and only analyzed the publicly available datasets from a previous publication (10).

Supplementary Information

The Supplementary File contains Supplementary Figures S1-S3 and their legends.

Figure legends

Figure 1 scRNAseq and scATACseq of d53 retina

(A) UMAP clustering of scRNAseq data generated seven clusters. (B) Characterization of each cluster with marker genes: CCND1 for MPCs, POU4F2 for RGC, and PLXNA2 for RPC. (C) DSL ligand expressions in each cluster. (D) NOTCH receptor expressions in each cluster. (E) The downstream target gene expressions in each cluster. (F) UMAP clustering of scATACseq data generated nine clusters. (G) Violin plot of the gene score (chromatin accessibility) for CCND1. Note that the two clusters (C3 and C4; arrowheads) had high scores. (H) Violin plot of the gene score for JAG1. Note the difference between the clusters C3 and C4. (G) Violin plot of the gene score for HES1.

Figure 2 scRNAseq and scATACseq of d59 retina

(A) UMAP clustering of scRNAseq data generated six clusters. (B) Characterization of each cluster with marker genes: CCND1 for MPCs, ELAVL4 for RGCs, PLXNA2 for RPC, CPLX2 for AMA, and OTX2 for CON/ROD. (C) DSL ligand expressions in each cluster. (D) NOTCH receptor expressions in each cluster. (E) The downstream target gene expressions in each cluster. (F) UMAP clustering of scATACseq data generated fifteen clusters. (G) Violin plot of the gene score for CPLX2. The cluster 14 was highlighted with the arrowheads. (H) Violin plot of the gene score for NOTCH1. (G) Violin plot of the gene score for HES5. Note the low level in the cluster 14.

Figure 3 scRNAseq and scATACseq of d78 retina

(A) UMAP clustering of scRNAseq data generated nine clusters. (B) Characterization of each cluster with marker genes: CCND1 for MPCs; OTX2 for CON/ROD; ELAVL4, PLXNA2 and MYBL1 for RGCs. (C) DSL ligand expressions in each cluster. (D) NOTCH receptor expressions in each cluster. (E) The downstream target gene expressions in each cluster. (F) UMAP clustering of scATACseq data generated ten clusters. (G) Violin plot of the gene score for CCND1. The cluster 6 was highlighted with the arrowheads. (H) Violin plot of the gene score for NOTCH1. (G) Violin plot of the gene score for HES1.

Figure1

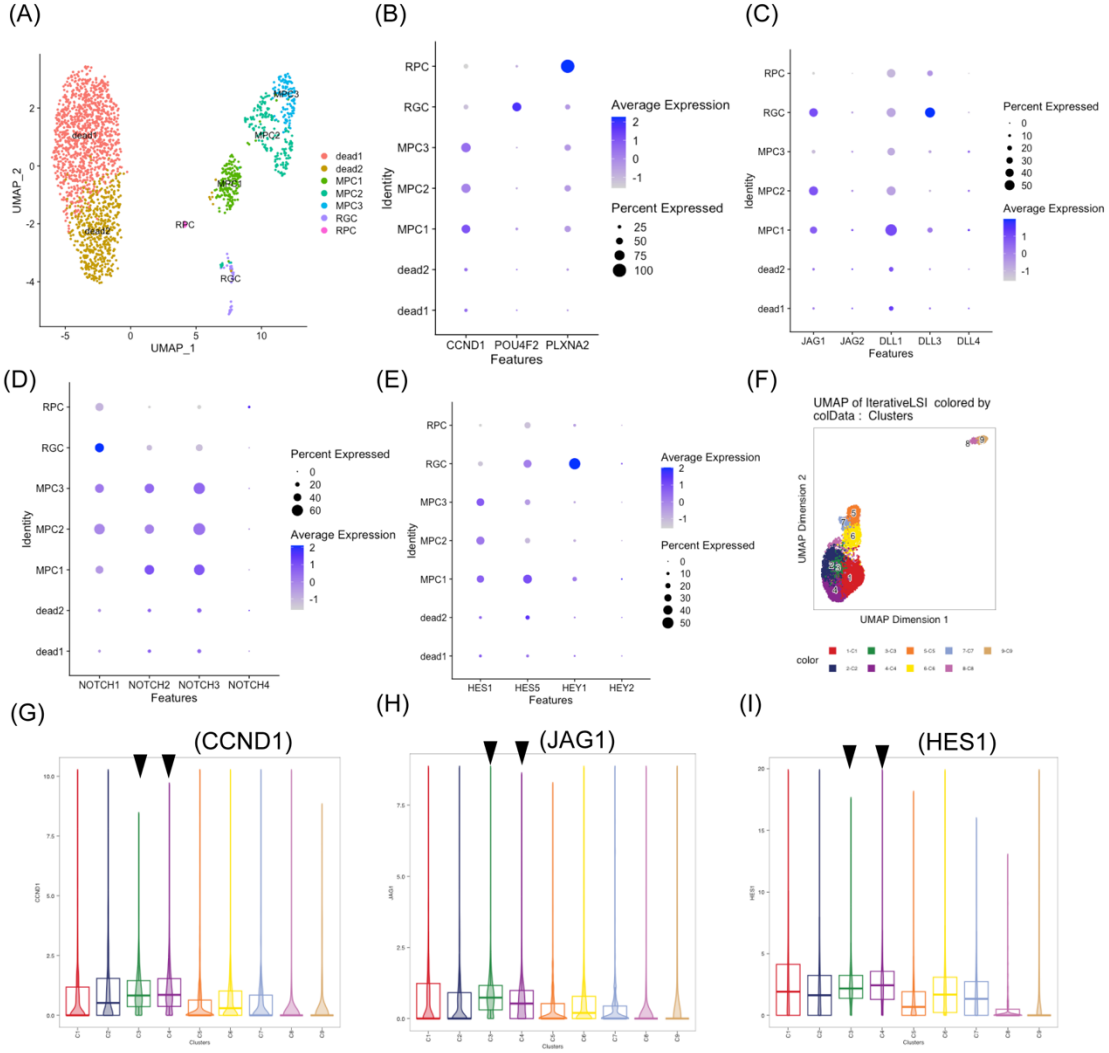
(A)
UMAP_2
UMAP_1
dead1
dead2
MPC1
MPC2
MPC3
RGC
RPC
(B)
Identity
Features
CCND1
POU4F2
PLXNA2
Average Expression
Percent Expressed
(C)
JAG1
JAG2
DLL1
DLL3
DLL4
(D)
NOTCH1
NOTCH2
NOTCH3
NOTCH4
(E)
HES1
HES5
HEY1
HEY2
(F)
UMAP of IterativeLSI colored by colData : Clusters
UMAP Dimension 1
UMAP Dimension 2
color
(G)
(CCND1)
(H)
(JAG1)
(I)
(HES1)

Figure 2

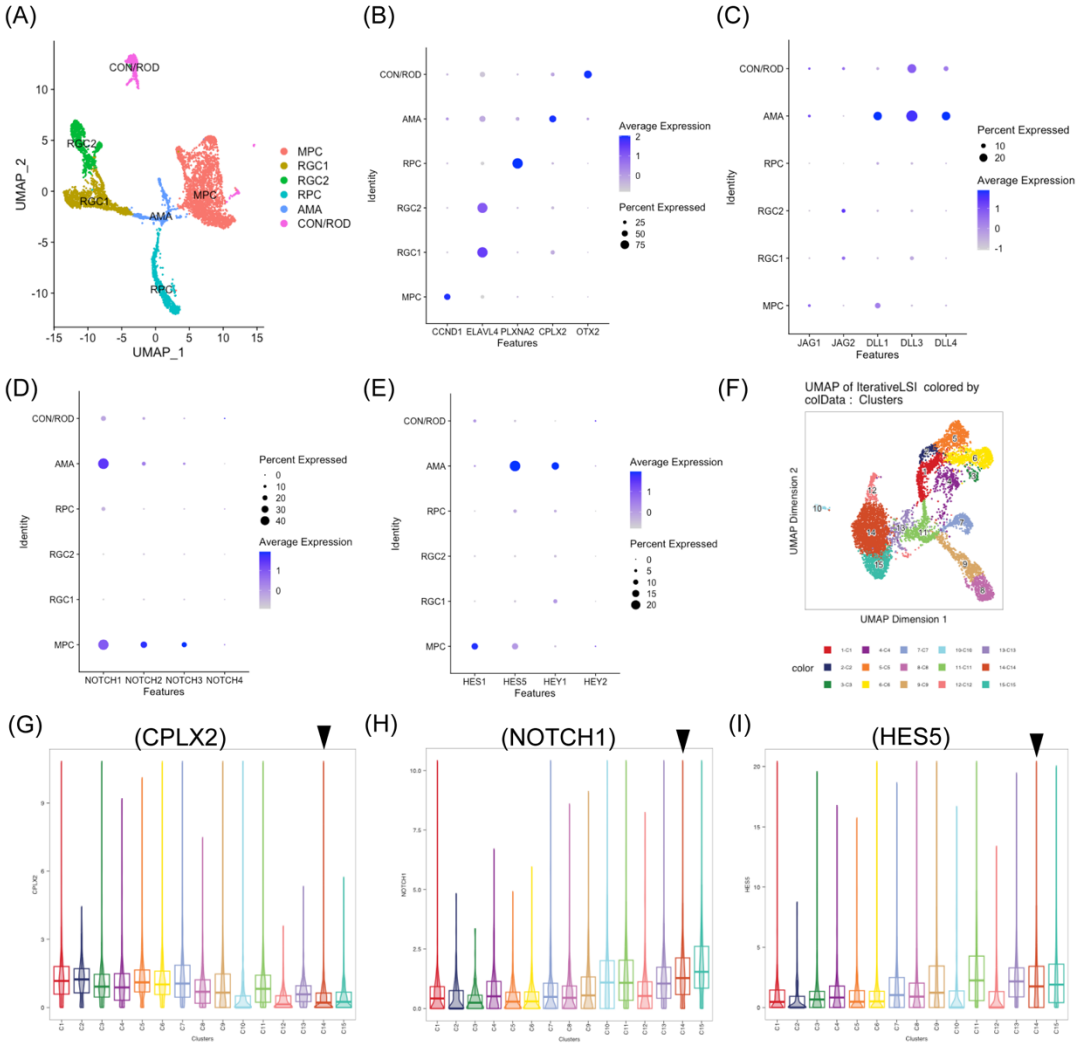
(A)
CON/ROD
RGC2
RGC1
MPC
AMA
RPC
UMAP_2
UMAP_1
MPC
RGC1
RGC2
RPC
AMA
CON/ROD
(B)
CON/ROD
AMA
RPC
RGC2
RGC1
MPC
Identity
CCND1 ELAVL4 PLXNA2 CPLX2 OTX2
Features
Average Expression
Percent Expressed
(C)
CON/ROD
AMA
RPC
RGC2
RGC1
MPC
Identity
JAG1 JAG2 DLL1 DLL3 DLL4
Features
Percent Expressed
Average Expression
(D)
CON/ROD
AMA
RPC
RGC2
RGC1
MPC
Identity
NOTCH1 NOTCH2 NOTCH3 NOTCH4
Features
Percent Expressed
Average Expression
(E)
CON/ROD
AMA
RPC
RGC2
RGC1
MPC
Identity
HES1 HES5 HEY1 HEY2
Features
Average Expression
Percent Expressed
(F)
UMAP of IterativeLSI colored by colData : Clusters
UMAP Dimension 2
UMAP Dimension 1
color
(G)
(CPLX2)
(H)
(NOTCH1)
(I)
(HES5)

Figure 3

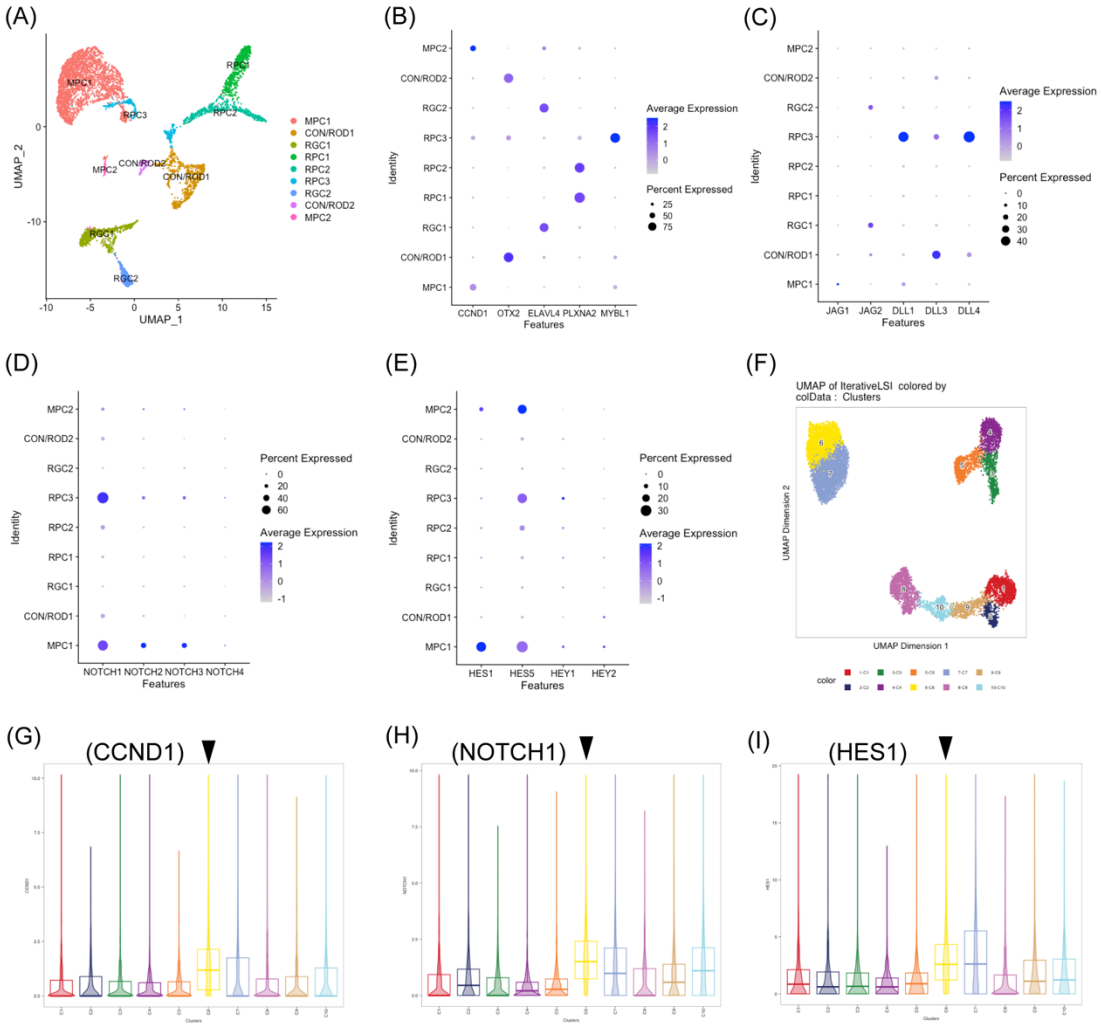
(A)
UMAP_1
UMAP_2
MPC1
CON/ROD1
RGC1
RPC1
RPC2
RPC3
RGC2
CON/ROD2
MPC2
(B)
Identity
Features
CCND1 OTX2 ELAVL4 PLXNA2 MYBL1
Average Expression
Percent Expressed
(C)
JAG1 JAG2 DLL1 DLL3 DLL4
(D)
NOTCH1 NOTCH2 NOTCH3 NOTCH4
(E)
HES1 HES5 HEY1 HEY2
(F)
UMAP of IterativeLSI colored by colData : Clusters
UMAP Dimension 1
UMAP Dimension 2
color
(G)
(CCND1)
(H)
(NOTCH1)
(I)
(HES1)

Figure1

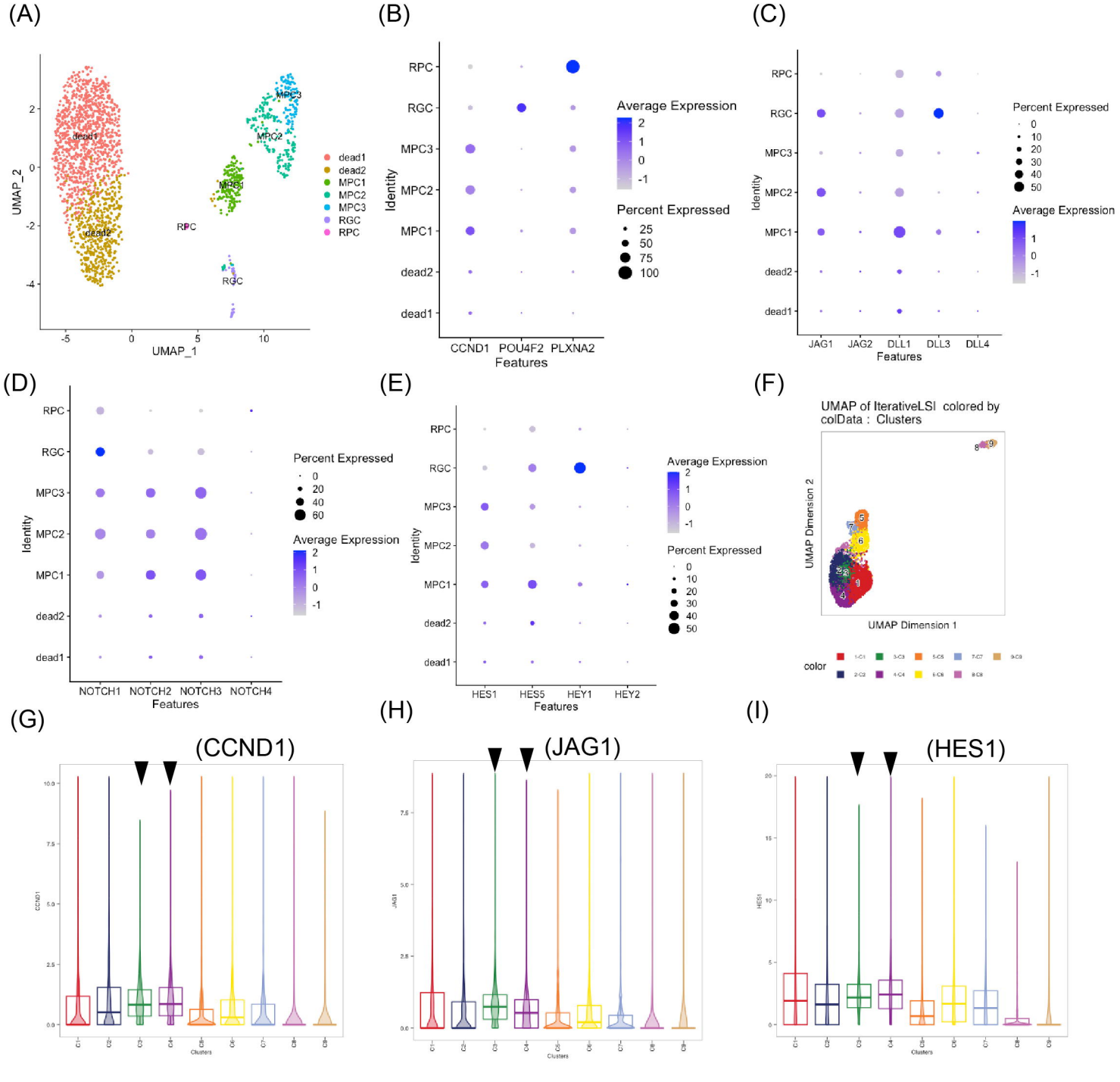
(A)
UMAP_2
UMAP_1
dead1
dead2
MPC1
MPC2
MPC3
RPC
RGC
(B)
Identity
Features
CCND1
POU4F2
PLXNA2
Average Expression
Percent Expressed
(C)
JAG1
JAG2
DLL1
DLL3
DLL4
(D)
NOTCH1
NOTCH2
NOTCH3
NOTCH4
(E)
HES1
HES5
HEY1
HEY2
(F)
UMAP of IterativeLSI colored by colData : Clusters
UMAP Dimension 1
UMAP Dimension 2
color
(G)
(CCND1)
(H)
(JAG1)
(I)
(HES1)

Figure 2

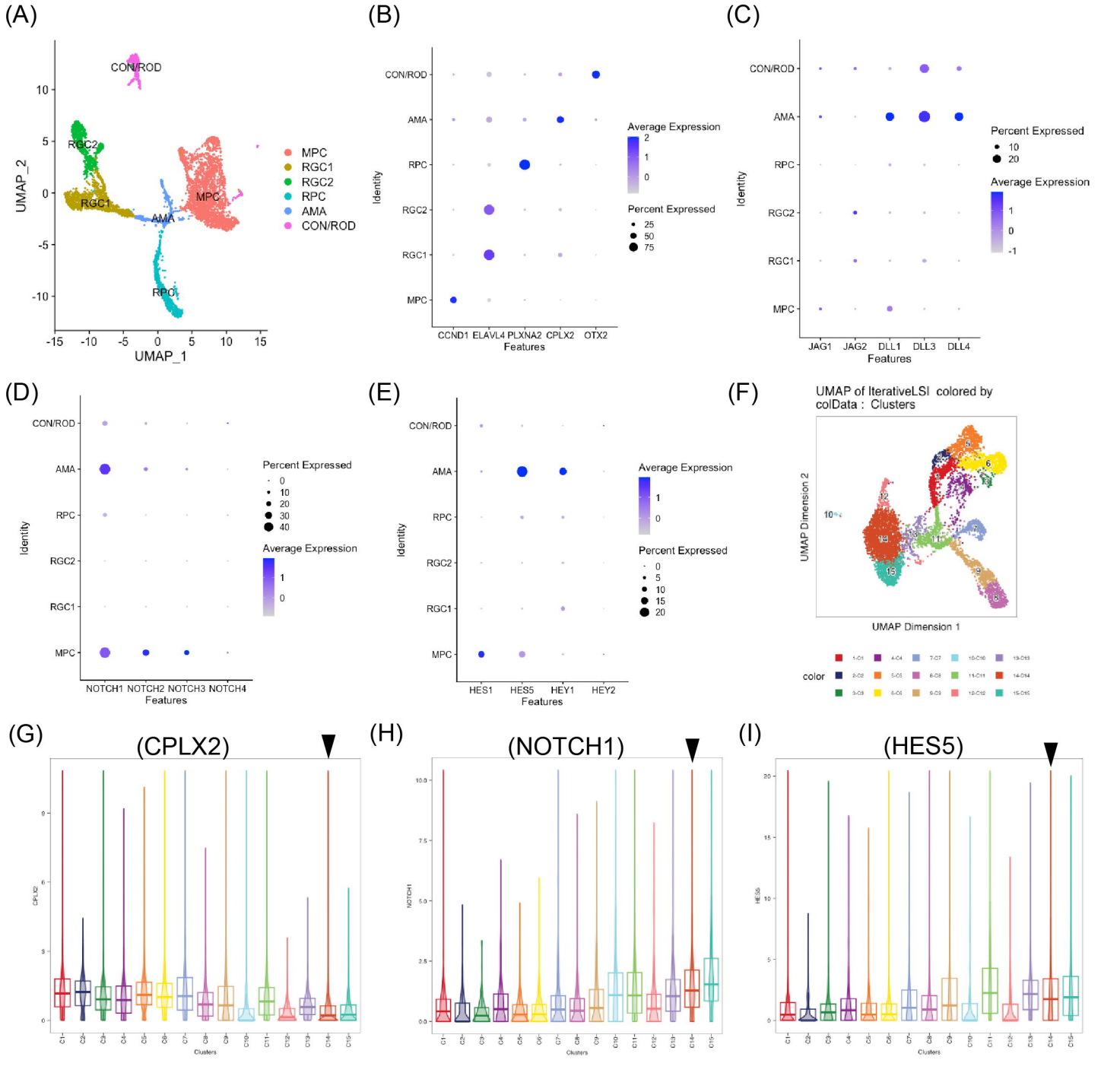
(A)
CON/ROD
RGC2
RGC1
MPC
AMA
RPC
UMAP_2
UMAP_1
MPC
RGC1
RGC2
RPC
AMA
CON/ROD
(B)
CON/ROD
AMA
RPC
RGC2
RGC1
MPC
Identity
CCND1 ELAVL4 PLXNA2 CPLX2 OTX2
Features
Average Expression
Percent Expressed
(C)
CON/ROD
AMA
RPC
RGC2
RGC1
MPC
Identity
JAG1 JAG2 DLL1 DLL3 DLL4
Features
Percent Expressed
Average Expression
(D)
CON/ROD
AMA
RPC
RGC2
RGC1
MPC
Identity
NOTCH1 NOTCH2 NOTCH3 NOTCH4
Features
Percent Expressed
Average Expression
(E)
CON/ROD
AMA
RPC
RGC2
RGC1
MPC
Identity
HES1 HES5 HEY1 HEY2
Features
Average Expression
Percent Expressed
(F)
UMAP of IterativeLSI colored by colData : Clusters
UMAP Dimension 2
UMAP Dimension 1
color
(G)
(CPLX2)
Clusters
(H)
(NOTCH1)
Clusters
(I)
(HES5)
Clusters

Figure 3

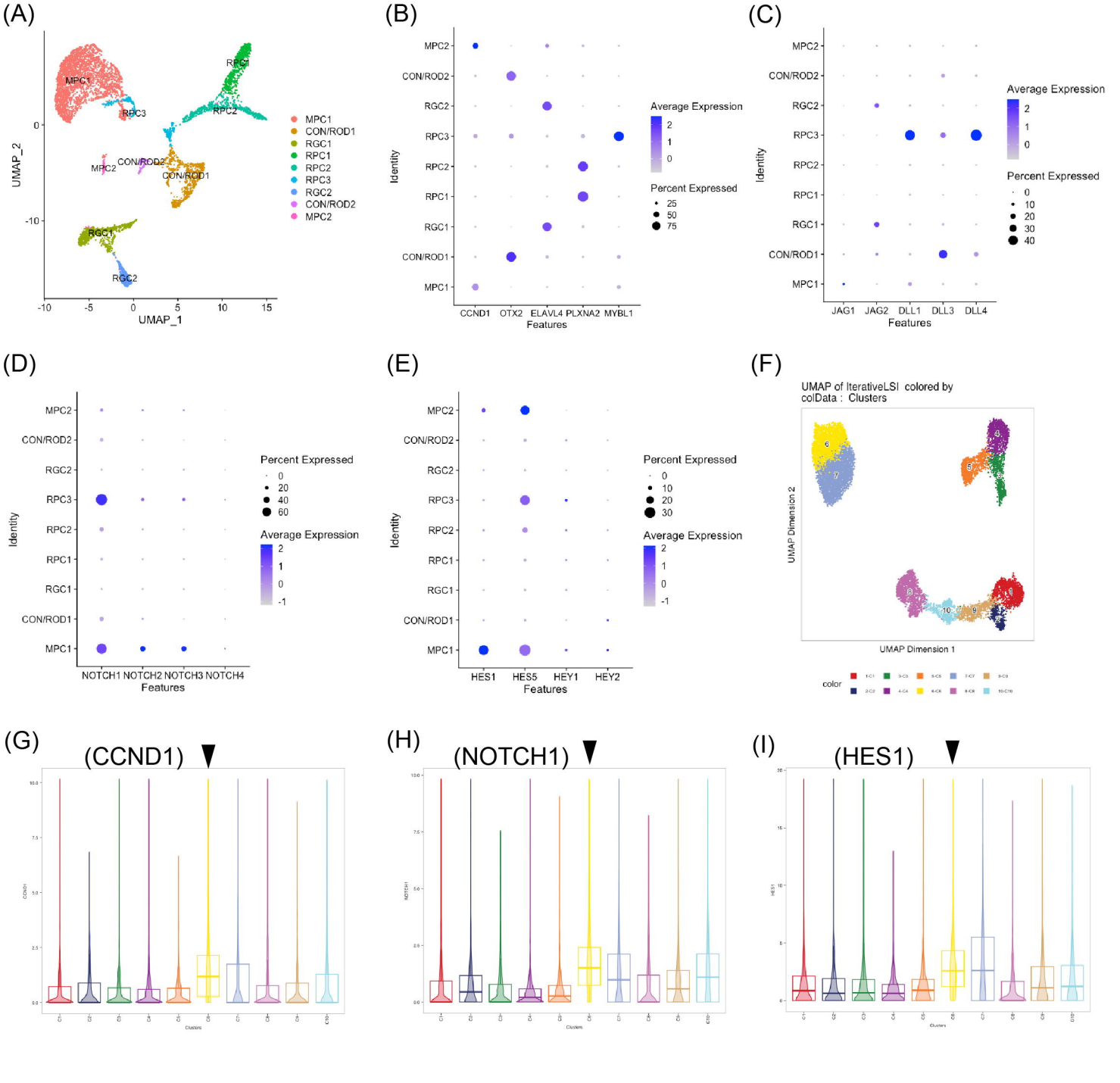
(A)
MPC1
RPC1
RPC3
RPC2
MPC2
CON/ROD2
CON/ROD1
RGC1
RGC2
UMAP_2
UMAP_1
MPC1
CON/ROD1
RGC1
RPC1
RPC2
RPC3
RGC2
CON/ROD2
MPC2
(B)
Identity
Features
CCND1 OTX2 ELAVL4 PLXNA2 MYBL1
Average Expression
Percent Expressed
(C)
Identity
Features
JAG1 JAG2 DLL1 DLL3 DLL4
Average Expression
Percent Expressed
(D)
Identity
Features
NOTCH1 NOTCH2 NOTCH3 NOTCH4
Percent Expressed
Average Expression
(E)
Identity
Features
HES1 HES5 HEY1 HEY2
Percent Expressed
Average Expression
(F)
UMAP of IterativeLSI colored by colData : Clusters
UMAP Dimension 1
UMAP Dimension 2
color
(G)
(CCND1)
(H)
(NOTCH1)
(I)
(HES1)